PHOTONICS Research

Kerr frequency combs in large-size, ultra-high-Q toroid microcavities with low repetition rates [Invited]

Jiyang Ma,[1] Xiaoshun Jiang,[1,*] and Min Xiao[1,2]

[1]National Laboratory of Solid State Microstructures, College of Engineering and Applied Sciences, and School of Physics, Nanjing University 210093, China
[2]Department of Physics, University of Arkansas, Fayetteville, Arkansas 72701, USA
*Corresponding author: jxs@nju.edu.cn

Received 21 July 2017; revised 26 October 2017; accepted 31 October 2017; posted 31 October 2017 (Doc. ID 302809); published 22 November 2017

By overcoming fabrication limitations, we have successfully fabricated silica toroid microcavities with both large diameter (of 1.88 mm) and ultra-high-Q factor (of 3.3×10^8) for the first time, to the best of our knowledge. By employing these resonators, we have further demonstrated low-threshold Kerr frequency combs on a silicon chip, which allow us to obtain a repetition rate as low as 36 GHz. Such a low repetition rate frequency comb can now be directly measured through a commercialized optical-electronic detector.

OCIS codes: (140.3945) Microcavities; (190.4390) Nonlinear optics, integrated optics; (190.4380) Nonlinear optics, four-wave mixing.

https://doi.org/10.1364/PRJ.5.000B54

1. INTRODUCTION

Optical frequency combs act as frequency "rulers," providing evenly spaced frequency lines. They have become useful tools in wide ranges of advanced scientific and applied fields [1–6]. The traditional optical frequency comb [1,2] is based on a large femtosecond mode-locked laser system that is difficult to integrate on a chip. Over the past decade, the rapid development of high-Q microresonators has led to the rise of a new type of optical frequency comb based on Kerr-nonlinearity, known as the Kerr comb [7,8]. Formed via the process of cascaded four-wave mixing, Kerr combs have been implemented in different kinds of microresonators [7]. Since their invention, Kerr combs have attracted tremendous attention and have been generated in several material systems [8–16], including several on-chip platforms [17–20]. On-chip operation is essential for integration with other optical components. Because of their small mode volumes and high-Q factors, these microresonator-based Kerr combs usually consume far less pump power, whereas typical threshold powers of several tens of microwatts have been reported for such optical frequency combs [8]. Because of their unique advantages over traditional optical frequency combs, as well as their potential for use in future applications, a number of significant studies have been conducted on such combs. These include comb noise characterization and dynamics [14], octave spanning [21,22], and time-domain characterizations, such as pulse shaping [19] and soliton formation inside the resonators [23,24]. In addition, Kerr combs have been demonstrated under various wavelength regimes, including visible light [25–30] and the near-infrared [8–16] to mid-infrared [31,32] ranges, each of which provides further potential for unique applications. Numerical simulations of Kerr combs have also been developed in depth [33,34]. One of the most significant applications of Kerr combs is providing a link between microwave and optical frequencies, such as in optical clocks [3,35]. To realize practical implementation in such cases, the comb needs to be fully stabilized [36]. Moreover, both a low repetition rate that is detectable with commercial detectors and octave spanning are required in the comb. A recent research study has shown that, by using silica disk resonators, one can achieve the lowest possible repetition rate of 2.6 GHz and near-octave comb spanning with a 66 GHz repetition rate [20].

Although the Kerr optical frequency comb was first achieved in silica toroid microcavities [8], due to the fabrication difficulty, microtoroid cavities are conventionally limited to low quality factors at large sizes [36]. As such, both the repetition rate and the threshold powers of the generated Kerr combs are quite high, which is undesirable for practical applications and makes this platform gradually unpopular in the community. In this paper, we present a method of producing low-threshold Kerr combs in large toroid cavities with diameters up to 1.88 mm and Q factors greater than 3×10^8. So far, the largest toroid cavity obtained in previously reported studies had a diameter of just 760 μm, and its corresponding optical Q factor was 2×10^7 [36] due to the fabrication limitations on large-diameter toroids. By optimizing the fabrication process,

we achieved ultra-high-Q millimeter scale toroid cavities with diameters and optical Q factors 2.5 and 16 times larger, respectively, than those of the previous results [36]. In addition, the cavities produced in our work possess higher optical Q factors than other ultra-high-Q on-chip silica disk microcavities of the same size [37]. In the following, we describe three large toroid cavities of different sizes and demonstrate the generated optical frequency combs in each of them.

2. DEVICE FABRICATION AND MEASURED RESULTS

The process of fabricating our cavities is similar to the method used in Ref. [38] and can be briefly described as follows. First, we use photolithography and buffered HF wet etching to pattern a silica disk onto a silicon wafer. Then, we undercut the silica disk using XeF_2 dry etching to ensure that the silica disk is supported by a circular silicon pedestal. Finally, we use a CO_2 laser to reflow the silica disk.

Usually, to ensure the silica disk is molten during the reflow process, the undercut of the disk should be deep enough, since the silicon pillar acts as a heat sink to the absorbed laser power. However, due to the large stress (especially for a large diameter silica disk) of the thermal oxide, deep undercut of the silica disk will make the disk buckle, featuring a crown-like pattern [39]. This effect is more serious for the larger diameter silica disk with a thinner thickness, which limits the fabrication of a silica toroid cavity with a large diameter.

To overcome this problem, here, we employ a thick oxide film (12 μm thickness) for the fabrication of large-diameter toroid cavities. Also, the thick thickness of the thermal oxide is helpful for the absorption of the CO_2 laser during the reflow process. During the experiment, the typical optical power of the CO_2 laser is 25–30 W. It is worth mentioning that, unlike repeating the reflow method of simply circulating the laser around the rim of the disk, as used in a previous study [36], when fabricating the toroid with a diameter of 514 or 800 μm, we illuminate the CO_2 laser over the whole surface of the disk so that its rim can be melted more evenly. However, when fabricating a toroid with a diameter of 1.88 mm, due to both the limited power of the CO_2 laser and the limited cross-sectional size of the laser beam, we circulate the laser around the disk's rim. Figure 1 shows scanning electron microscopy (SEM) images of our large toroid resonators. The principle and minor diameters of the three fabricated toroid cavities are 514 μm, 800 μm, and 1.88 mm; and 81.4, 78.7, and 70.6 μm, respectively. Accordingly, their calculated mode volumes for the fundamental TE-like cavity mode are 3.2×10^{-14}, 5.5×10^{-14}, and 22.8×10^{-14} m^3, respectively [40].

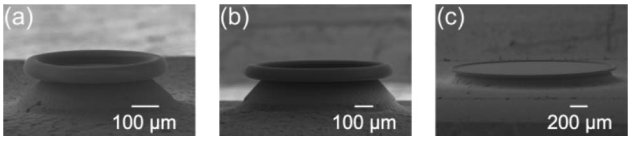

Fig. 1. SEM images of toroid cavities: (a) cavity with principle diameter of 514 μm, (b) cavity with principle diameter of 800 μm, and (c) cavity with principle diameter of 1.88 mm.

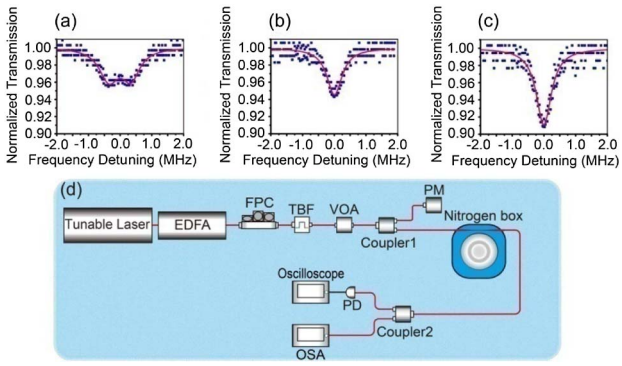

Fig. 2. (a) Transmission spectrum of toroid cavity with a diameter of 514 μm and the corresponding intrinsic Q factor of 2.7×10^8; (b) transmission spectrum of a cavity with diameter of 800 μm and the corresponding intrinsic Q factor of 3.0×10^8; (c) transmission spectrum of cavity with a diameter of 1.88 mm and the corresponding intrinsic Q factor of 3.3×10^8; (d) experimental setup. EDFA, erbium doped fiber amplifier; FPC, fiber polarization controller; TBF, tunable bandpass filter; VOA, variable optical attenuator; PM, powermeter; PD photodiode; and OSA, optical spectrum analyzer.

We test our sample's Q factor, threshold power, and comb formation using the setup shown in Fig. 2(d). The Q factor of our sample is determined by first transmitting the scanned laser (with a linewidth of ~200 kHz) into the cavity through a tapered fiber and then measuring the full width at half-maximum of the transmitted Lorentz peak using an oscilloscope. The intrinsic Q factors are measured to be 2.7×10^8, 3.0×10^8, and 3.3×10^8 for cavities with diameters of 514 μm, 800 μm, and 1.88 mm, respectively, as shown in Figs. 2(a)–2(c). The achieved optical Q factors and the diameters of the toroid cavities are 16.5 and 2.5 times larger, respectively, than the ones reported in the previous work [36]. Also, these measured optical Q factors are ~3.0, 1.7, and 1.2 times larger than the wet-etched silica disk cavities with similar diameters [20,37]. To the best of our knowledge, our cavities have the highest Q factors among all the reported on-chip silica microresonators of the same sizes.

3. DISPERSION SIMULATION

Before generating optical frequency combs, we calculate the dispersion of our toroid cavities through the finite-element-simulation method with COMSOL 4.3 software [40]. The dispersion can be determined via the detuning of the cavity's two adjacent free spectral ranges (FSRs), which we define as

$$\Delta\mathrm{FSR} = (\nu_{m+1} - \nu_m) - (\nu_m - \nu_{m-1}) = \nu_{m+1} + \nu_{m-1} - 2\nu_m. \quad (1)$$

We can also describe the dispersion as [8]

$$D \approx \frac{\Delta\mathrm{FSR} \times 4\pi^2 n^3 R^2}{c^2 \lambda^2}, \quad (2)$$

where R stands for the radius of the cavity. In Figs. 3(a) and 3(b), we show the calculated dispersions of these three cavities. It is clear that all three cavities possess anomalous dispersions ($D > 0$) under the 1550 nm wavelength regime, which is advantageous for the generation of Kerr combs.

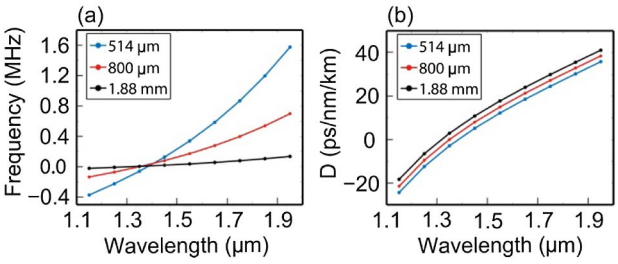

Fig. 3. (a) Calculated dispersions represented as ΔFSR and (b) calculated dispersions represented as D (in ps/nm/km).

4. THRESHOLD POWER MEASUREMENT

Then, we measure the thresholds of optical parametric oscillation of our toroid cavities. As shown in Fig. 4, the measured threshold powers for toroid cavities with diameters of 514 μm, 800 μm, and 1.88 mm are 330, 508, and 980 μW, respectively, under their own coupling conditions. These values are lower than the threshold powers of both on-chip silica disks and toroids at similar sizes due to the increased Q factors [20,36]. According to previous studies [14], the formula for the threshold power of optical parametric oscillation in a whispering gallery mode cavity can be written as

$$P_{\mathrm{th}} = \frac{V_0 n_0^2 \omega}{8 n_2 c \eta Q^2}, \tag{3}$$

where V_0 denotes the effective mode volume, n_0 represents the linear refractive index of silica, ω is the pump laser's angular frequency, n_2 is the nonlinear refractive index of silica, η is the coupling rate, c is the speed of light in vacuum, and Q represents the total Q factor of the pump mode. By substituting parameters into Eq. (3), the calculated threshold values match well with the experimental data.

5. KERR COMB GENERATION

Next, we illustrate the dynamic comb-generation process as we tune the wavelength from just inside the resonance mode toward the resonance point. During this process we use the thermal lock method [41] to ensure that the wavelength does not shift away, and to achieve mechanical stability, we attach a tapered fiber to the cavity so that the coupling rate between the cavity and the fiber remains constant during the process. Naturally, all three

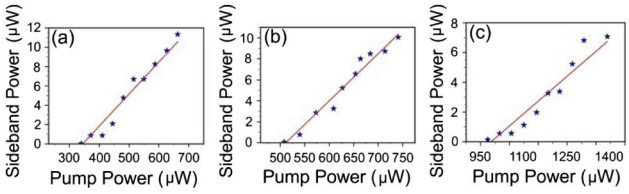

Fig. 4. (a) Measured threshold power of toroid with diameter of 514 μm, loaded Q factor of 8.5×10^7, and corresponding coupled pump power of 330 μW. (b) Measured threshold power of toroid with diameter of 800 μm, loaded Q factor of 2.4×10^8, and corresponding coupled pump power of 508 μW. (c) Measured threshold power of toroid with diameter of 1.88 mm, loaded Q factor of 1.7×10^8, and corresponding coupled pump power of 980 μW.

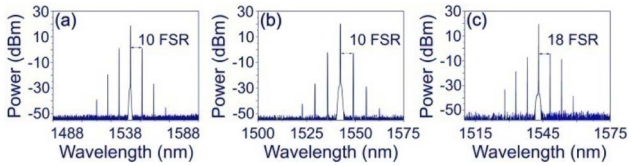

Fig. 5. First comb lines excited for (a) 514 μm toroid, first comb line excited 10 FSR away from the central mode; (b) 800 μm toroid, first comb line excited 10 FSR away from the central mode; and (c) 1.88 mm toroid, first comb line excited 18 FSR away from the central mode.

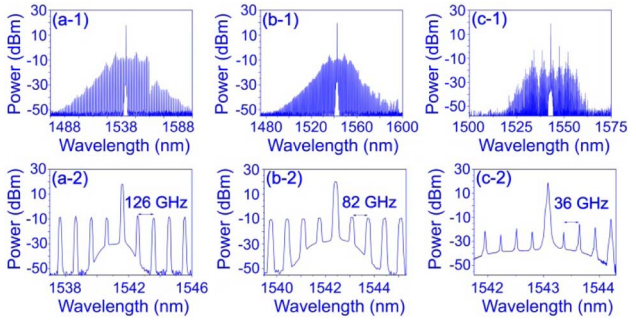

Fig. 6. Spectra of optical combs: (a-1) optical frequency comb in toroid with diameter of 514 μm, and corresponding repetition rate of 126 GHz; (a-2) closeup of nine comb lines around the pump mode; (b-1) optical frequency comb in toroid with diameter of 800 μm, and corresponding repetition rate of 82 GHz; (b-2) closeup of nine comb lines around the pump mode; (c-1) optical frequency comb in toroid with diameter of 1.88 mm, and corresponding repetition rate of 36 GHz; (c-2) closeup of nine comb lines around the pump mode.

cavities operate in the over-coupled regime. As Fig. 5 illustrates, in each of these cases, the first comb line is not excited in the mode adjacent to the pump mode and that corresponds to a Turing pattern comb [34]. The first line to become excited can be simulated by the method presented in Refs. [33,34].

Figure 6 shows the measured spectra of the generated frequency comb using an optical spectrum analyzer with a resolution of 0.02 nm. The numbers of comb lines are 118, 149, and 146 with coupled pump powers of 15.4, 18.7, and 20.1 mW, respectively, for resonators with diameters of 514 μm, 800 μm, and 1.88 mm. In the cavities with diameters of 800 μm and 1.88 mm, the combs have repetition rates of 82 and 36 GHz, respectively, which can be detected directly with a commercial detector and is very useful when locking methods are used to attempt to stabilize the comb [36]. To our knowledge, in the structure of the silica toroid microcavities, the 36 GHz repetition rate is the lowest repetition rate that has ever been achieved.

6. CONCLUSIONS

We demonstrated the generation of optical frequency combs in large toroid microresonators of different sizes whose Q factors exceeded 3.0×10^8 and whose diameters reached as large as

1.88 mm. The threshold power of our biggest device was lower than 1 mW with a repetition rate of 36 GHz, which, to the best of our knowledge, is the smallest repetition rate ever achieved in a silica toroid cavity. A commercial detector was able to detect this value directly, which better facilitates its practical applications. In future studies, we will analyze the noise of the combs in our cavities and attempt to stabilize the combs by locking the pump lasers, both in amplitude and frequency, and generate the solitons. Beyond the generation of the frequency comb, such large toroid cavities with ultra-high-Q factor can also be very useful in demonstrating narrow-linewidth Brillouin lasers, on-chip frequency stabilization, and gyroscopes.

Funding. National Key R&D Program of China (2017YFA0303703, 2016YFA0302500); National Natural Science Foundation of China (NSFC) (61435007, 11574144, 61475099); Natural Science Foundation of Jiangsu Province, China (BK20150015); Fundamental Research Funds for the Central Universities (021314380086).

REFERENCES

1. T. Udem, R. Holzwarth, and T. W. Hänsch, "Optical frequency metrology," Nature **416**, 233–237 (2002).
2. D. J. Jones, S. A. Diddams, J. K. Ranka, A. Stentz, R. S. Windeler, J. L. Hall, and S. T. Cundiff, "Carrier-envelope phase control of femtosecond mode-locked lasers and direct optical frequency synthesis," Science **288**, 635–639 (2000).
3. S. A. Diddams, T. Udem, J. C. Bergquist, E. A. Curtis, R. E. Drullinger, L. Hollberg, W. M. Itano, W. D. Lee, C. W. Oates, K. R. Vogel, and D. J. Wineland, "An optical clock based on a single trapped $^{199}Hg^{+}$ ion," Science **293**, 825–828 (2001).
4. R. Holzwarth, T. Udem, T. W. Hänsch, J. C. Knight, W. J. Wadsworth, and P. St.J. Russell, "Optical frequency synthesizer for precision spectroscopy," Phys. Rev. Lett. **85**, 2264–2267 (2000).
5. S. A. Diddams, J. C. Bergquist, S. R. Jefferts, and C. W. Oates, "Standards of time and frequency at the outset of the 21st century," Science **306**, 1318–1324 (2004).
6. T. Steinmetz, T. Wilken, C. Araujo-Hauck, R. Holzwarth, T. W. Hänsch, L. Pasquini, A. Manescau, S. D'Odorico, M. T. Murphy, T. Kentischer, W. Schmidt, and T. Udem, "Laser frequency combs for astronomical observations," Science **321**, 1335–1337 (2008).
7. T. J. Kippenberg, R. Holzwarth, and S. A. Diddams, "Microresonator-based optical frequency combs," Science **332**, 555–559 (2011).
8. P. Del'Haye, A. Schliesser, O. Arcizet, T. Wilken, R. Holzwarth, and T. J. Kippenberg, "Optical frequency comb generation from a monolithic microresonator," Nature **450**, 1214–1217 (2007).
9. A. A. Savchenkov, A. B. Matsko, V. S. Ilchenko, I. Solomatine, D. Seidel, and L. Maleki, "Tunable optical frequency comb with a crystalline whispering gallery mode resonator," Phys. Rev. Lett. **101**, 093902 (2008).
10. I. S. Grudinin, N. Yu, and L. Maleki, "Generation of optical frequency combs with a CaF_2 resonator," Opt. Lett. **34**, 878–880 (2009).
11. S. B. Papp and S. A. Diddams, "Spectral and temporal characterization of a fused-quartz-microresonator optical frequency comb," Phys. Rev. A **84**, 053833 (2011).
12. B. J. M. Hausmann, I. Bulu, V. Venkataraman, P. Deotare, and M. Lonar, "Diamond nonlinear photonics," Nat. Photonics **8**, 369–374 (2014).
13. H. Jung, C. Xiong, K. Y. Fong, X. Zhang, and H. X. Tang, "Optical frequency comb generation from aluminum nitride microring resonator," Opt. Lett. **38**, 2810–2813 (2013).
14. T. Herr, K. Hartinger, J. Riemensberger, C. Y. Wang, E. Gavartin, R. Holzwarth, M. L. Gorodetsky, and T. J. Kippenberg, "Universal formation dynamics and noise of Kerr-frequency combs in microresonators," Nat. Photonics **6**, 480–487 (2012).
15. M. A. Foster, J. S. Levy, O. Kuzucu, K. Saha, M. Lipson, and A. L. Gaeta, "Silicon-based monolithic optical frequency comb source," Opt. Express **19**, 14233–14239 (2011).
16. Q. Lu, S. Liu, X. Wu, L. Liu, and L. Xu, "Stimulated Brillouin laser and frequency comb generation in high-Q microbubble resonators," Opt. Lett. **41**, 1736–1739 (2016).
17. J. S. Levy, A. Gondarenko, M. A. Foster, A. C. Turner-Foster, A. L. Gaeta, and M. Lipson, "CMOS-compatible multiple-wavelength oscillator for on-chip optical interconnects," Nat. Photonics **4**, 37–40 (2010).
18. L. Razzari, D. Duchesne, M. Ferrera, R. Morandotti, S. Chu, B. E. Little, and D. J. Moss, "CMOS-compatible integrated optical hyperparametric oscillator," Nat. Photonics **4**, 41–45 (2010).
19. F. Ferdous, H. Miao, D. E. Leaird, K. Srinivasan, J. Wang, L. Chen, L. T. Vargheses, and A. M. Weiner, "Spectral line-by-line pulse shaping of on-chip microresonator frequency combs," Nat. Photonics **5**, 770–776 (2011).
20. J. Li, H. Lee, T. Chen, and K. J. Vahala, "Low-pump-power, low-phase-noise, and microwave to millimeter-wave repetition rate operation in microcombs," Phys. Rev. Lett. **109**, 233901 (2012).
21. P. Del'Haye, T. Herr, E. Gavartin, M. L. Gorodetsky, R. Holzwarth, and T. J. Kippenberg, "Octave spanning tunable frequency comb from a microresonator," Phys. Rev. Lett. **107**, 063901 (2011).
22. Y. Okawachi, K. Saha, J. S. Levy, Y. H. Wen, M. Lipson, and A. L. Gaeta, "Octave-spanning frequency comb generation in a silicon nitride chip," Opt. Lett. **36**, 3398–3400 (2013).
23. T. Herr, V. Brasch, J. D. Jost, C. Y. Wang, N. M. Kondratiev, M. L. Gorodetsky, and T. J. Kippenberg, "Temporal solitons in optical microresonators," Nat. Photonics **8**, 145–152 (2014).
24. X. Yi, Q.-F. Yang, K. Y. Yang, M.-G. Suh, and K. Vahala, "Soliton frequency comb at microwave rates in a high-Q silica microresonator," Optica **2**, 1078–1085 (2015).
25. A. A. Savchenkov, A. B. Matsko, W. Liang, V. S. Ilchenko, D. Seidel, and L. Maleki, "Kerr combs with selectable central frequency," Nat. Photonics **5**, 293–296 (2011).
26. S. Miller, K. Luke, Y. Okawachi, J. Cardenas, A. L. Gaeta, and M. Lipson, "On-chip frequency comb generation at visible wavelengths via simultaneous second- and third-order optical nonlinearities," Opt. Express **22**, 26517–26525 (2014).
27. S. H. Lee, D. Y. Oh, Q.-F. Yang, B. Shen, H. Wang, K. Y. Yang, Y. H. Lai, X. Yi, and K. Vahala, "Towards visible soliton microcomb generation," arXiv:1705. 06703v2 (2017).
28. X. Guo, C.-L. Zou, H. Jung, Z. Gong, A. Bruch, L. Jiang, and H. X. Tang, "Efficient visible frequency comb generation via Cherenkov radiation from a Kerr microcomb," arXiv:1704. 04264v1 (2017).
29. H. Jung, R. Stoll, X. Guo, D. Fischer, and H. X. Tang, "Green, red, and IR frequency comb line generation from single IR pump in AlN microring resonator," Optica **1**, 396–399 (2014).
30. Y. Yang, X. Jiang, S. Kasumie, G. Zhao, L. Xu, J. M. Ward, L. Yang, and S. N. Chormaic, "Four-wave mixing parametric oscillation and frequency comb generation at visible wavelengths in a silica microbubble resonator," Opt. Lett. **41**, 5266–5269 (2016).
31. C. Y. Wang, T. Herr, P. Del'Haye, A. Schliesser, J. Hofer, R. Holzwarth, T. W. Hänsch, N. Picque, and T. J. Kippenberg, "Mid-infrared optical frequency combs at 2.5 μm based on crystalline microresonators," Nat. Commun. **4**, 1345 (2013).
32. A. G. Griffith, R. K. W. Lau, J. Cardenas, Y. Okawachi, A. Mohanty, R. Fain, Y. H. D. Lee, M. Yu, C. T. Phare, C. B. Poitras, A. L. Gaeta, and M. Lipson, "Silicon-chip mid-infrared frequency comb generation," Nat. Commun. **6**, 6299 (2015).
33. Y. K. Chembo and N. Yu, "Modal expansion approach to optical-frequency-comb generation with monolithic whispering-gallery-mode resonators," Phys. Rev. A **82**, 033801 (2010).
34. C. Godey, I. V. Balakireva, A. Coillet, and Y. K. Chembo, "Stability analysis of the spatiotemporal Lugiato-Lefever model for Kerr optical frequency combs in the anomalous and normal dispersion regimes," Phys. Rev. A **89**, 063814 (2014).
35. S. B. Papp, K. Beha, P. Del'Haye, F. Quinlan, H. Lee, K. J. Vahala, and S. A. Diddams, "Microresonator frequency comb optical clock," Optica **1**, 10–14 (2014).

36. P. Del'Haye, O. Arcizet, A. Schliesser, R. Holzwarth, and T. J. Kippenberg, "Full stabilization of a microresonator-based optical frequency comb," Phys. Rev. Lett. **101**, 053903 (2008).
37. H. Lee, T. Chen, J. Li, K. Y. Yang, S. Jeon, O. Painter, and K. J. Vahala, "Chemically etched ultrahigh-Q wedge-resonator on a silicon chip," Nat. Photonics **6**, 369–373 (2012).
38. D. K. Armani, T. J. Kippenberg, S. M. Spillane, and K. J. Vahala, "Ultra-high-Q toroid microcavity on a chip," Nature **421**, 925–928 (2003).
39. T. Chen, H. Lee, and K. Vahala, "Thermal stress in silica-on-silicon disk resonators," Appl. Phys. Lett. **102**, 031113 (2013).
40. M. Oxborrow, "Traceable 2D finite-element simulation of the whispering-gallery modes of axisymmetric electromagnetic resonators," IEEE Trans. Microwave Theory Tech. **55**, 1209–1218 (2007).
41. T. Carmon, L. Yang, and K. J. Vahala, "Dynamical thermal behavior and thermal self-stability of microcavities," Opt. Express **12**, 4742–4750 (2004).